

The Magnetic Microstructure of Nanostructured Materials

Rudolf Schäfer

IFW Dresden, Inst. f. Metallic Materials,
Helmholtzstr. 20, D-01069 Dresden
r.schaefer@ifw-dresden.de

A review is given on the magnetic microstructure and magnetization processes of modern fine- and nanocrystalline magnetic materials, based on Kerr-microscopical domain observation. The grain size dependence of coercivity together with typical domain images is summarized in Fig. 1. In coarse-grained material the domain character is determined by the surface orientation of the individual grains [1]. The rising influence of grain boundary domains with decreasing grain size is responsible for the characteristic $1/D$ dependence of coercivity. For grain sizes in the 100 nm regime, coercivity shows a maximum that can be applied for hard magnets. Immobile, patchy domains are characteristic for this regime. With further decreasing grain size, coercivity drastically falls off with D^6 , leading to extremely soft magnetic nanocrystalline and finally amorphous material. Residual anisotropies in competition with controllable, macroscopic anisotropies are responsible for the domain character in such materials [1, 2].

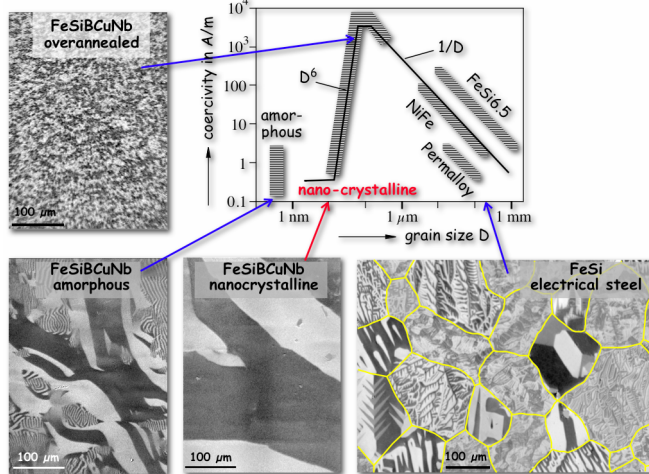


Fig. 1 Coercivity as function of grain size (after [3]) for a number of materials, together with typical domain images

1. Domains in nanocrystalline ribbons

Nanocrystalline FeCuNbSiB ribbons, produced by rapid quenching and annealing, reveal a homogeneous ultrafine grain structure of bcc FeSi with grain sizes of typically 10–15 nm and random orientation, embedded in an amorphous minority matrix [3]. The microstructure leads to a distribution of magnetic anisotropy axes randomly varying their orientation over the scale of the grain size D (Fig. 2). As D is smaller than the ferromagnetic correlation length L_{ex} , the smoothing action of exchange energy impedes the magnetization to follow the local anisotropy axes, i.e. local anisotropies are largely washed out. As the average random anisotropy is negligibly small, the domains are controlled by uniaxial ani-

sotropies (like field- or creep induced anisotropies) that are uniform on a macroscopic scale. Apparently homogeneously magnetized domains (see Fig. 1) are therefore observed [4]. The size of uniaxial anisotropy can be controlled by field annealing (also annealing without magnetic field will cause induced anisotropy along the direction of local magnetization of the domains present during annealing).

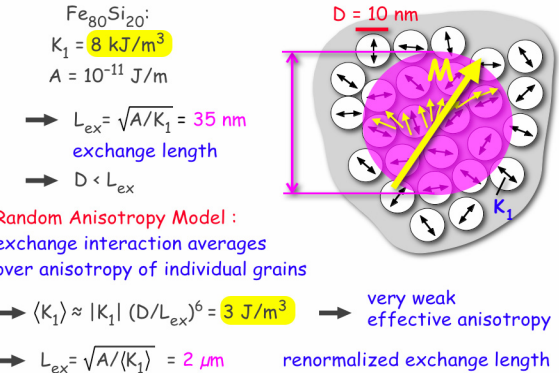


Fig. 2 Visualization of the random anisotropy model in nanocrystalline material. The exchange length L_{ex} represents the characteristic minimum scale below which the direction of magnetization cannot vary appreciably (A and K_1 are exchange and magnetocrystalline anisotropy constants, respectively)

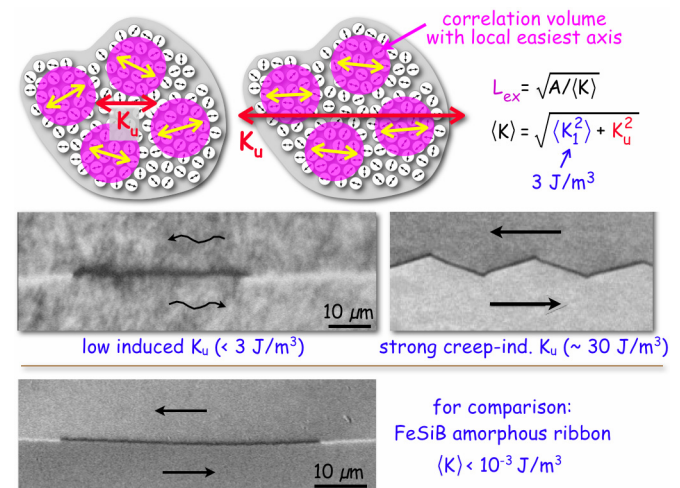


Fig. 3 The interplay of effective random ($\square K_1 \square$) and induced (K_u) anisotropy determines the degree of magnetization modulation on a microscopic scale. Shown are high-resolution observations on $\text{Fe}_{73}\text{Cu}_1\text{Nd}_3\text{Fe}_{16}\text{B}_7$ nanocrystalline ribbons (20 μm thick) with different strengths of induced anisotropy, as well as an amorphous ribbon for comparison

On a microscopic scale, however, interesting details are revealed that depend on the competition of random and uniform (induced) anisotropy (Fig. 3) [5, 6]. If the uniform anisotropy is larger than the effective random anisotropy, the domains are homogeneously magnetized also on a microscopic scale. For induced anisotropies in the order of or lower than the effective random anisotropy, the magnetization is microscopically modulated in a patch-like way within otherwise regular domains that are oriented along the induced anisotropy direction. These patches are fluctuating on a scale of a few micrometers which is the order of the renormalized ex-

change length (see Fig. 2). They reflect the angular dispersion of the easiest magnetic axis (given by statistical fluctuations) from one correlation volume to the other.

Domain modulations on the microscopic scale have consequences for magnetization processes (Fig. 4). Whereas for weak modulation (i.e. strong induced anisotropy) the easy axis process is governed by domain wall motion, nucleation-dominated processes are observed for strong modulation (i.e. small induced anisotropy) due to the strong microscopic disorder in magnetization. Correspondingly, homogeneous and inhomogeneous rotational processes, respectively, are observed in hard-axis fields. The modulation has also a strong impact on the dynamic magnetization processes at elevated frequencies. A nucleation-dominated process is observed for strongly modulated material (Fig. 5), while wall motion is found in higher anisotropy material (not shown). In both cases, the domain refinement with increasing frequency is caused by eddy current effects. Interestingly, the material with the smallest induced anisotropy (i.e. strongest modulation) reveals the highest permeability and lowest power loss.

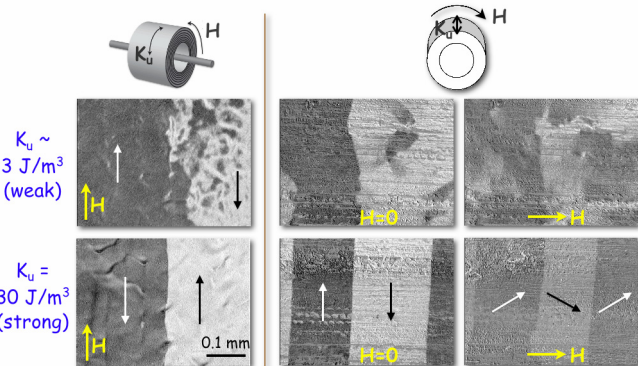


Fig. 4 Easy-axis (left) and hard-axis (right) magnetization processes for two different nanocrystalline FeCuNdFeB ring cores with circumferential and transverse induced anisotropy axis, respectively, of different strengths.

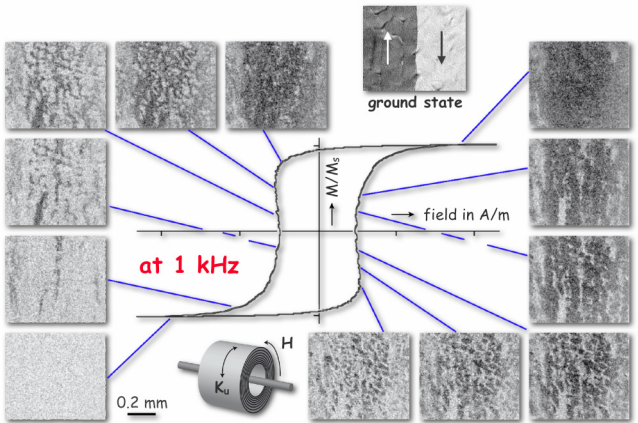


Fig. 5 Stroboscopic observation of the dynamic easy-axis process at 1 kHz on a low-anisotropy nanocrystalline ring core. The regular 180° domains of the ground state are replaced by patch domains at high frequency (after [7]).

According to the random anisotropy model [3], the effective anisotropy constant $\square K_1 \square$ is equal to $|K_1| \sqrt{N}$, where K_1 is the magnetocrystalline anisotropy and N is

the number of exchange-coupled grains within the re-normalized correlation volume. Consequently, the magnetic microstructure of nanocrystalline ribbons can be modified by either changing K_1 (Fig. 6a, b) or N (Fig. 6c). If the random anisotropy is less effectively averaged out, a patchy and immobile domain structure is observed.

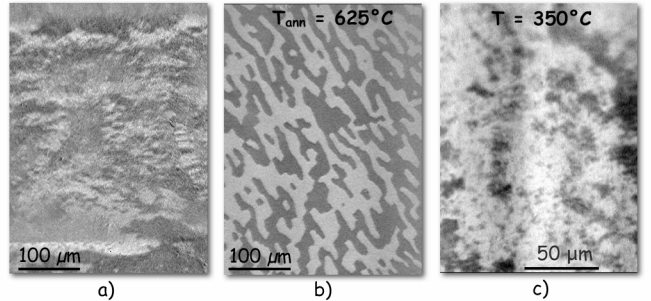


Fig. 6 (a) Adding cobalt to the standard FeCuNdFeB alloy significantly increases the magnetocrystalline anisotropy, leading to a stronger effective anisotropy and immobile patch domains. The $\text{Co}_{45}\text{Fe}_{28.5}\text{Si}_{13.5}\text{B}_9\text{Cu}_1\text{Nd}_3$ ribbon was provided by Pilar Marin, Madrid. Patchy domains are also observed in (b), where a regular FeCuNdFeB ribbon was “overannealed”. Here Fe_2B precipitates have been formed that have a high magnetocrystalline anisotropy, thus increasing the effective anisotropy although the grain size of the bcc FeSi grains remains unchanged. Image (c) shows patch domains in an optimized FeCuNdFeB ribbon that was heated above the Curie point of the amorphous matrix phase, leading to a reduction of the number of exchange coupled grains (after [6]).

2. Domains in nanocrystalline magnetic films

When nanocrystalline ribbons are thinned to the micrometer regime and below (Fig. 7), the patchy modulation of magnetization changes to a classical ripple pattern with a textured modulation that is well known from thin film magnetism [1]. This indicates that both, ripple and patches are due to the statistical perturbation by the crystal anisotropy, caused by the irregular nanocrystalline microstructure in each case.

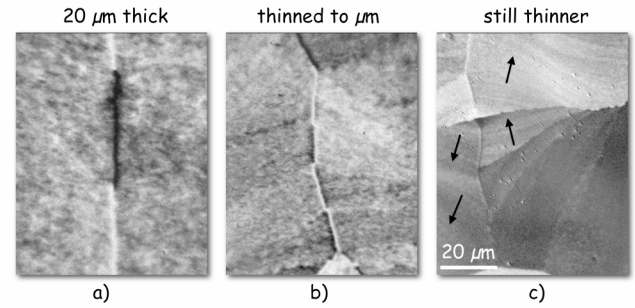


Fig. 7 (a) Patch-like modulated domains in nanocrystalline $\text{Fe}_{84}\text{Zr}_{3.5}\text{Nb}_{3.5}\text{B}_8\text{Cu}_1$ ribbon (thickness 20 μm), which transform into ripple (b, c) by thinning the ribbon (after [2]).

The preference of a textured modulation in the case of films and a patchy modulation for bulk nanocrystalline material, respectively, can be explained by stray field arguments (Fig. 8). Consider two neighborhoods of grains (correlation volumes), in which by statistical fluctuations two local anisotropy axes dominate that are superimposed onto an average (induced) anisotropy axis.

If the two neighborhoods are magnetized along different angles ϑ_1 and ϑ_2 , a “transverse” magnetic charge $\lambda_{\text{trans}} = \sin \vartheta_1 - \sin \vartheta_2$ is generated at the supposed boundary. For small ϑ this charge is much larger than the longitudinal charge $\lambda_{\text{lon}} = \cos \vartheta_1 - \cos \vartheta_2$ appearing at the boundary of longitudinally neighbored areas. The stray field energy therefore suppresses lateral variations of magnetization, thus causing ripple texture orthogonal to the average anisotropy axis. This discussion is based on the fact that in thin films the magnetization vector is forced parallel to the film plane by the demagnetizing field. In bulk material, there is the additional freedom of magnetization modulation also in the third dimension. If one correlation volume is magnetized to the left, there can be another one underneath that is magnetized to the right. This leads to a cancellation of transverse magnetization components so that stray fields, which would enforce certain wall orientations, are irrelevant. Arbitrarily oriented walls, i.e. patch domains, are the consequence.

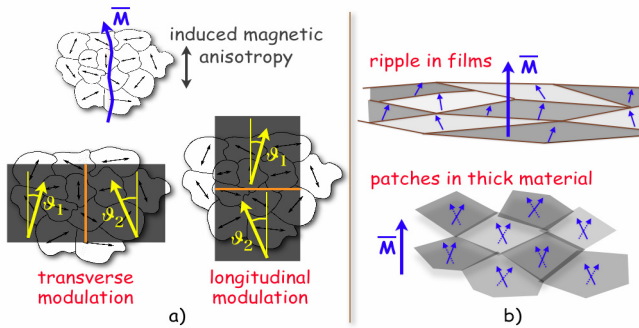


Fig. 8 (a) Stray field argument in favor of longitudinal magnetization ripple in magnetic films. (b) The cancellation of transverse magnetization allows a patchy modulation in case of bulk nanocrystalline material like ribbons. A macroscopic, induced anisotropy, here aligned vertically, was assumed.

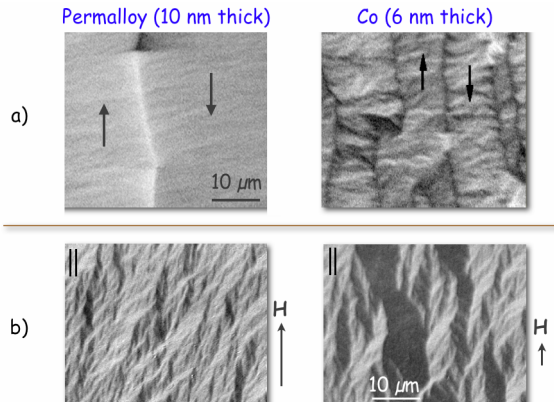


Fig. 9 (a) Polycrystalline Co films with strong magnetocrystalline anisotropy show a stronger ripple effect than Permalloy. (b) The large microscopic dispersion in Co-films leads to a nucleation dominated magnetization process – shown are two domain states in decreasing magnetic field, observed on a 6 nm thick Co-film. All films were prepared by sputtering, thus having a nanocrystalline microstructure

The same arguments as for the nanocrystalline ribbons also apply to films: A stronger magnetocrystalline anisotropy leads to less-effective averaging effects, i.e. a stronger microscopic dispersion of magnetization. Consequently, Permalloy films with their very small crystal

anisotropy show a much weaker ripple effect than cobalt films (Fig. 9a). In the latter a strongly nucleation-dominated magnetization process is observed (Fig. 9b).

3. Domains in fine- and nanostructured permanent magnets

The microstructure of common permanent magnets like hexaferrites, NdFeB or CoSm type magnets consists of highly anisotropic grains in the size range of 10 μm in a polycrystalline, textured compound that are prepared in such a way, that the switching of one grain has little influence on its neighbors [1]. Regular domains are observed in such material, the character of which depends on the orientation of the observed surface. But permanent magnets can also be prepared from *single-domain* particles. Classical examples are the *Alnico* alloys, consisting of fine filaments of a high-saturation FeCo alloy that are embedded into a non-magnetic NiAl matrix.

Modern small particle magnets are based on high-anisotropy materials that consist of single-domain *grains*. A number of techniques can be used to prepare fine-crystalline magnets out of precursors such as Nd₂Fe₁₄B [8]: rapid quenching and subsequent crystallization, mechanical alloying, and the HDDR-process. All these methods generate a fine powder with a particle size around 100 μm and a grain size between some 10 nm and some 100 nm, which then has to be compacted into solid magnets. Oriented magnets can be produced by “die-upsetting”. Also by the HDDR process an anisotropic powder can be produced which can be oriented in a magnetic field.

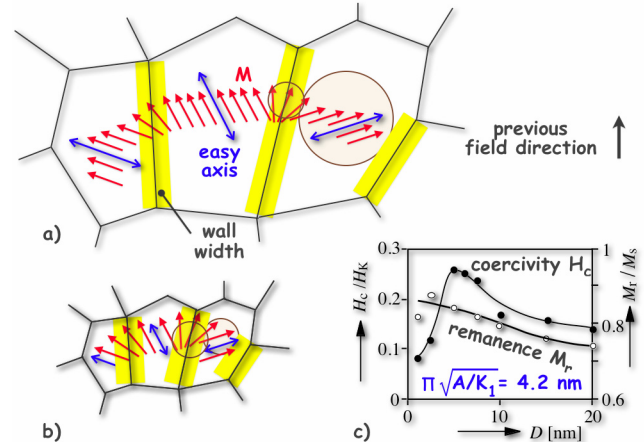


Fig. 10 Mechanism of remanence-enhancement in non-oriented, nanocrystalline NdFeB magnets. The rotational zones around the grain boundaries in the order of the domain wall width contribute to the remanence. Their relative volume increases with decreasing grain size [compare (a) and (b)]. Simulated coercivity and remanence curves are shown in (c) (taken from [9]).

But even non-oriented nano-crystalline materials remain interesting as a relatively weak exchange interaction between very small grains can lead to an enhanced remanence without a significant loss in coercivity (exchange enhanced magnets). The coupling enhances the remanence above the average $M_r = 0.5 M_s$ of independently oriented uniaxial grains (see Fig. 10). A further

possibility of achieving high remanence in non-oriented nanocrystalline materials consists in adding a high-saturation soft magnetic phase, which is strongly exchange coupled to the basic hard magnetic phase if the extension of the soft phase is sufficiently small. The coercivity in these two-phase nano-crystalline magnets is dominated by the hard phase, whereas the high remanence is primarily a consequence of the soft phase. A highly irregular magnetic microstructure that is modulated on the scale of the grain size (i.e. of the order of some ten nanometers) is found in such material. It somehow resembles the irregular patch domains of the over-annealed FeCuNbSiB ribbons (see Fig. 1), although on a much finer scale due to the higher anisotropy and smaller grain size.

If the exchange coupling between single-domain grains is interrupted, the dipolar interaction between the grains causes *magnetostatic interaction domains* [1] (Figs. 12, 13). They are characterized by grain neighborhoods, in which all grains are correlatively saturated along their individual easy axis along a certain net direction. Interaction domains are the more pronounced the better the texture of the material [12]. Interestingly, such domains have recently also been found in the classical Sm₂Co₁₇ pinning magnets, which indicates predominant magnetostatic interaction between the Sm₂(CoFe)₁₇ cells that are interrupted by precipitation phases [13].

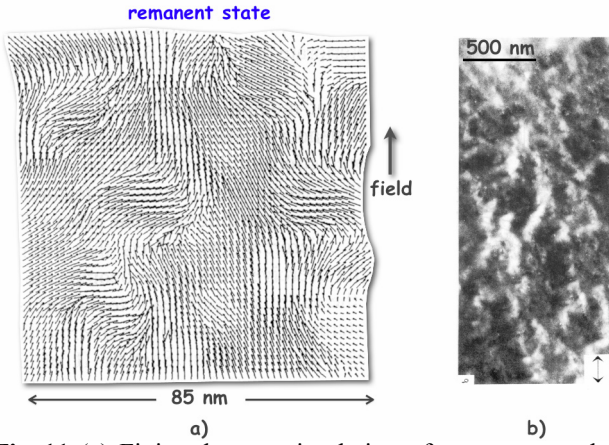


Fig. 11 (a) Finite element simulation of remanence-enhanced Nd₂Fe₁₄B/Fe₃B magnet (taken from [10]). (b) Domain image, obtained by transmission electron microscopy in the Foucault mode, of Nd₂Fe₁₄B/Fe material (taken from [11]).

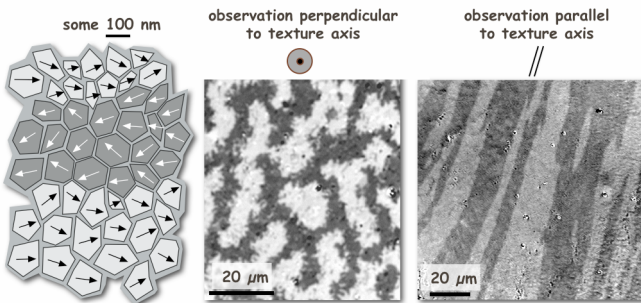


Fig. 12 Magnetostatic interaction domains in fine-crystalline NdFeB material, where the Nd₂Fe₁₄B-grains are exchange-decoupled by a paramagnetic grain boundary phase

Note that the „softening-effect“ due to random anisotropy as described in Chap. 1 is irrelevant for nanos-

tructured permanent magnets, even in the case of exchange-coupled grains. The exchange length L_{ex} is 1.3 nm in NdFeB (with K_u = 4.3·10⁶ kJ/m³ and A = 8·10⁻¹² J/m), being far below the typical grain size of 20 nm.

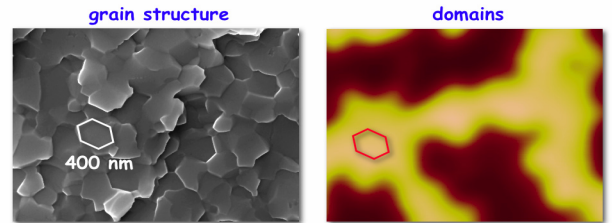


Fig. 13 The comparison between grain structure and interaction domains (here imaged by Magnetic Force Microscopy) directly proves, that the domains extend over several correlated grains (courtesy O. Gutfleisch, taken from [14])

Bibliography

- [1] A. Hubert and R. Schäfer: *Magnetic Domains. The Analysis of Magnetic Microstructures*. Springer, Berlin (1998)
- [2] R. Schäfer: *Domains in extremely soft magnetic materials*. J. Magn. Magn. Mat. **215-216**, 652-663 (2000)
- [3] G. Herzer, *Nanocrystalline soft magnetic alloys*. In: Buschow K.H.J., editor. *Handbook of Magnetic Materials*, vol. 10. Elsevier Science B.V., p.415 (1997)
- [4] R. Schäfer, A. Hubert, G. Herzer: *Domain observation on nanocrystalline material*. J. Appl. Phys. **69**, 5325 (1991)
- [5] G. Herzer: *Anisotropies in soft magnetic nanocrystalline alloys*. J. Magn. Magn. Mat. **294**, 99-106 (2005)
- [6] S. Flohrer, R. Schäfer, Ch. Polak, G. Herzer: *Interplay of uniform and random anisotropy in nanocrystalline soft magnetic alloys*. Acta Materialia **53**, 2937-2942 (2005)
- [7] S. Flohrer, R. Schäfer, J. McCord, S. Roth, G. Herzer, L. Schultz: *Magnetization loss and domain refinement in nanocrystalline tape wound cores*. Acta. Mat. **54**, 3253-3259 (2006)
- [8] O. Gutfleisch, A. Bollero, A. Handstein, D. Hinz, A. Kirchner, A. Yan, K.-H. Müller, L. Schultz: *Nanocrystalline high performance magnets*, J. Magn. Magn. Mat. **242-245**, 1277-1283 (2002)
- [9] W. Rave and K. Ramstöck: *Micromagnetic calculation of the grain size dependence of remanence and coercivity in nanocrystalline permanent magnets*, J. Magn. Magn. Mat. **171**, 69-82, (1997)
- [10] T. Schrefl and J. Fidler: *Finite element modeling of nanocomposite magnets*. IEEE Trans. Magn. **35**, 3223 (1999)
- [11] J.N. Chapman, S. Young, H.A. Davies, P. Zhang, A. Mafaf, R.A. Buckley: *A TEM investigation of the magnetic domain structure in nanocrystalline NdFeB samples*. Proc. 13th Int. Workshop on RE Magnets & their applications, p.95, Birmingham (1994)
- [12] K. Khlopkov, O. Gutfleisch, R. Schäfer, D. Hinz, K.-H. Müller, L. Schultz: *Interaction domains in die-upset NdFeB magnets in dependence on the degree of deformation*. J. Magn. Magn. Mat. **272-276**, E1937-E1939 (2004)
- [13] O. Gutfleisch, K.-H. Müller, K. Khlopkov, M. Wolf, A. Yan, R. Schäfer, T. Gemming, L. Schultz: *Evolution of magnetic domain structures and coercivity in high-performance SmCo 2:17 type permanent magnets*, Acta Materialia **54**, 997-1008 (2006)
- [14] K. Khlopkov, O. Gutfleisch, D. Hinz, K.-H. Müller and L. Schultz, "Evolution of interaction domains with texture in Nd₂Fe₁₄B studied with magnetic force microscopy", J. Appl. Phys., accepted.